ACS APPLIED MATERIALS & INTERFACES

Research Article

www.acsami.org

Neuropeptide Y Y_1 Receptors Meditate Targeted Delivery of Anticancer Drug with Encapsulated Nanoparticles to Breast Cancer Cells with High Selectivity and Its Potential for Breast Cancer Therapy

Juan Li,[†] Zheyu Shen,[†] Xuehua Ma,[†] Wenzhi Ren,[†] Lingchao Xiang,[†] An Gong,[†] Tian Xia,[‡] Junming Guo,[‡] and Aiguo Wu*[,†]

[†]Key Laboratory of Magnetic Materials and Devices & Division of Functional Materials and Nano Devices, Ningbo Institute of Materials Technology & Engineering, Chinese Academy of Sciences, Ningbo 315201, China

[‡]Department of Biochemistry and Molecular Biology, Zhejiang Provincial Key Laboratory of Pathophysiology, Ningbo University School of Medicine, Ningbo 315211, China

Supporting Information

ABSTRACT: By enabling nanoparticle-based drug delivery system to actively target cancer cells with high selectivity, active targeted molecules have attracted great attention in the application of nanoparticles for anticancer drug delivery. However, the clinical application of most active targeted molecules in breast cancer therapy is limited, due to the low expression of their receptors in breast tumors or coexpression in the normal and tumor breast tissues. Here, a neuropeptide Y Y_1 receptors ligand PNBL-NPY, as a novel targeted molecule, is conjugated with anticancer drug doxorubicin encapsulating albumin nanoparticles to investigate the effect of Y_1 receptors on the delivery of drug-loaded nanoparticles to breast cancer cells and its potential for breast cancer therapy. The PNBL-NPY can actively recognize and bind to the Y_1 receptors that are significantly overexpressed on the surface of the breast cancer cells, and the drug-loaded nanoparticles are delivered directly into the cancer cells through internalization. This system is highly selective and able to distinguish the breast cancer cells from the normal cells, due to normal breast cells that express Y_2 receptors only. It is anticipated that this study may provide a guidance in the development of Y_1 receptor-based nanoparticulate drug delivery system for a safer and more efficient breast cancer therapy.

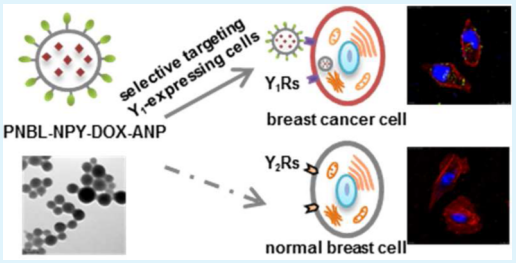

KEYWORDS: *Y_1 receptors, [Pro^{30}, Nle^{31}, Bpa^{32}, Leu^{34}]NPY(28−36), targeted delivery, albumin nanoparticles, breast cancer*

INTRODUCTION

Proper targeting is one of the key issues in the development of anticancer drug delivery system, requiring that the anticaner drug reaches the targeted area and efficiently induces its pharmacological action without damaging healthy tissues.[1] Active targeted molecules, such as ligands or antibodies, have been conjugated with nanoparticle systems to improve the targetbility of anticancer drug, due to their receptors being overexpressed in tumors.[2−7] However, the application of most targeted molecules in breast cancer therapy is limited, because their receptors are either expressed in lower incidence in breast tumors, such as folate receptors (∼29%) and integrin receptors (∼26%),[8,9] or concomitantly in the normal and tumor breast tissues, such as vasoactive intestinal peptide receptors and gastrin-releasing peptide receptors.[10,11] Therefore, the application of such targeted molecules might result in less therapeutic effect and some side effects in breast cancer therapy.

Recently, it has been identified that neuropeptide Y receptors are highly overexpressed in human breast tumors, but the expressed subtype between tumor breast and normal breast tissues are different.[12,13] Y_1 subtype receptors (Y_1Rs) are overexpressed in 90% human breast tumors and in 100% of the examined metastases, whereas normal human breast tissues express Y_2 subtype receptors (Y_2Rs) preferentially. Additionally, neoplastic transformation can switch the neuropeptide Y receptors expression from Y_2 to Y_1 subtype.[13] Hence, we hypothesize that the selective ligand of Y_1Rs might be used as a potential targeted molecule, mediating the delivery of drug-encapsulated nanoparticles into breast cancer cells with high selectivity and minimized damage to normal breast tissues. Until now, some neuropeptide Y analogues have been labeled or modified with different radiometal or chelating agent combinations, to obtain stable compounds with selective Y_1 binding for positron emission tomography (PET) diagnosis of breast cancer.[14−17] However, it is currently unclear whether Y_1Rs could meditate the targeted delivery of anticancer drug-loaded nanoparticles for breast cancer therapy.

Received: January 10, 2015
Accepted: February 19, 2015
Published: February 19, 2015

DOI: 10.1021/acsami.5b00270
ACS Appl. Mater. Interfaces 2015, 7, 5574−5582

Nanocarriers are widely used in the development of anticancer drug delivery.[18−23] Owing to their high surface area-to-volume ratio, it is possible to achieve high ligand density on the surface for targeting purposes. In this study, albumin nanoparticles were adopted as a shuttle for anticancer drug delivery, due to their good stability, solubility, biodegradability, and the lack of toxicity and immunogenicity.[24] Anticancer drugs, such as doxorubicin or paclitaxel, have been encapsulated to albumin nanoparticles and conjugated with galactosamine or folic acid to improve their targetability.[25,26] To date, some albumin-anticancer drug conjugates have been evaluated clinically.[27,28] Especially, an albumin paclitaxel nanoparticle (Abraxane) has been proved in 2005 by FDA for treating metastatic breast cancer.[29] In our lab, the prepared albumin nanoparticles have the property of autofluorescence,[25,30,31] which facilitates the evaluation of cellular uptake by either laser scanning confocal microscope (LSCM) or flow cytometry. Additionally, the solvents that we use to prepare the albumin nanoparticles are ethanol and phosphate buffer solution (PBS), and the desolvation process is easy to scale up.

Herein, we conjugated a highly selective Y_1R_S ligand [Pro^{30}, Nle^{31}, Bpa^{32}, Leu^{34}]NPY(28−36)^{32} with anticancer drug doxorubicin (DOX)-loaded albumin nanoparticles (ANP), which is abbreviated hereafter as PNBL-NPY-DOX-ANP, to investigate the effect of Y_1Rs on the delivery of anticancer drug-encapsulated nanoparticles to breast cancer cells and its potential for breast cancer therapy. The DOX-ANP were prepared in a single step by using a desolvation technique coupled with chemical cross-linking by glutaraldehyde, and then the PNBL-NPY was conjugated onto the surface of the ANP in the presence of 1-ethyl-3-(3-(dimethylamino)propyl) carbodiimide (EDAC). LSCM imaging and flow cytometry analysis were performed to evaluate the cellular uptake of the prepared nanoparticles in human breast cancer MCF-7 cell line previously shown to highly express Y_1Rs.[13,33] Because Y_1Rs are overexpressed on human breast tumors, while normal human breast tissues express Y_2Rs preferentially,[13,34] the cellular uptake difference between human breast cancer cells MCF-7 and human normal breast cells MCF-10A was checked. To address whether PNBL-NPY-modified DOX-ANP could potentially be used for breast cancer therapy, the cytotoxicity of the prepared nanoparticles was evaluated by MTT assays for MCF-7 cells. In addition, previous studies have reported that neuropeptide Y and its analogues could affect the cell proliferation; for instance, neuropeptide Y could inhibit the growth of human neuronal epithelioma cells SK-N-MC.[13] In this case, the effect of PNBL-NPY ligand on the cell viability of MCF-7 cells was also tested in our study.

EXPERIMENTAL SECTION

Materials. Bovine serum albumin (BSA), glutaraldehyde (50 wt %), and DOX hydrochloride were purchased from Sigma-Aldrich (Shanghai, China). EDAC, *N*-hydroxysuccinimide (NHS), L-lysine (Lys), sodium chloride (NaCl), 3-(4,5-dimethylthiazol-2-yl)-2,5-diphenyltetrazolium bromide (MTT), sodium hydroxide (NaOH, 99.99%), ethanol, and dimethyl sulfoxide (DMSO) were purchased from Sinopharm Chemical Reagent Co., Ltd. (Shanghai, China). [Pro^{30}, Nle^{31}, Bpa^{32}, Leu^{34}]NPY(28−36) (IIe-Asn-Pro-Nle-Bpa-Arg-Leu-Arg-Try-NH_2) was synthesized by the LifeTein LLC (Beijing, China). Rhodamine phalloidin (RP) and Hoechst 33342 were purchased from Invitrogen (Carlsbad, U.S.). Acetonitrile and trifluoroacetic acid (TFA) were purchased as HPLC grade from Aladdin Industrial Inc. (Shanghai, China).

Preparation of PNBL-NPY Modified DOX-ANP. DOX-encapsulating ANP was prepared according to reported methods.[25] Ethanol (6.0 mL) was dropwise added into 2.0 mL of BSA/DOX aqueous solution (500 μg mL^{-1} DOX and 20 mg mL^{-1} BSA in 10 mM NaCl solution at pH 10.8) and stirred at room temperature for ∼2 min. Immediately after ethanol addition, 80 μL of 8% glutaraldehyde aqueous solution was rapidly charged to induce cross-linking. The cross-linking process was continued overnight under stirring. Lys (1.0 mL) aqueous solution (40 mg mL^{-1}) was then introduced to end-cap the free aldehyde groups on the surface of nanoparticles. After 1.0 h of reaction, the suspensions were centrifuged (11 500 g, 15 min) and washed three times with Milli-Q water to obtain the purified DOX-loaded ANP (DOX-ANP) without free aldehyde groups on surface. The supernatant was ultrafiltered for DOX concentration test by using UV detection at a wavelength of 480 nm, and the solid was lyophilized for the yield calculation. In the end, the drug loading content (DLC) and drug loading efficiency (DLE) were calculated by using the following equations:

$$\text{drug-loading content (DLC\%)} = \frac{\text{weight of DOX in ANP}}{\text{weight of ANP}} \times 100$$

$$\text{drug-loading efficiency (DLE\%)} = \frac{\text{weight of DOX in ANP}}{\text{weight of the feeding DOX}} \times 100$$

To conjugate PNBL-NPY ligand onto the surface of DOX-ANP, an ice-cooled DOX-ANP (1 mg mL^{-1} in PBS) was activated by a mixture solution of EDAC (0.3 mg mL^{-1}) and NHS (0.2 mg mL^{-1}) solution for 0.5 h. Then 1.0 mL of ice-cooled PNBL-NPY (1.0 mg mL^{-1} in PBS) solution was added into 9 mL of activated DOX-ANP (1 mg mL^{-1} in PBS) solution, and the mixture was stirred at room temperature for 16 h. The resulting PNBL-NPY-DOX-ANP was centrifuged (12 500 g, 15 min), and the supernatants were stored for further analysis. Unreacted PNBL-NPY remaining in the supernatant was lyophilized and concentrated with acetonitrile and water (1:1, v/v). An HPLC-UV 2695/2998 system (Waters, U.S.) was used for the quantification of PNBL-NPY. A C_{18} column (4.6 mm × 250 mm, 5 μm) was used to separate PNBL-NPY from other interference. Mobile phase A was an aqueous solution containing 0.1% TFA, and mobile phase B was acetonitrile containing 0.1% TFA. The analysis was performed using a gradient profile with mobile phase B increased from 9.0% to 60% (0.0−20.0 min). The column was reconditioned using a 9.0% solution of mobile phase B for 10 min before further injection. The flow rate was 1 mL min^{-1}, and a sample of 20 μL was injected in the column each time. The peak area (wavelength = 220 nm) of the supernatant was converted into a PNBL-NPY concentration by using a calibration curve constructed with standard PNBL-NPY solutions (Supporting Information, Figure S2). A simple mass balance was then used to calculate the amount of PNBL-NPY conjugation on the surface of DOX-ANP.

Size and Zeta Potential Analysis and Transmission Electron Microscopy. Particle size and size distribution of the nanoparticle dispersions were measured at room temperature by dynamic light scattering (DLS) using a Zeta particle size analyzer (Nano-ZS, Malvern, England). The data were collected on an autocorrelator with a detection angle of scattered light of 173°.

To obtain detailed structural and morphological information, ∼1 μL of the diluted nanoparticle dispersion was dropped onto a copper grid coated with a thin layer of carbon film and then dried at room temperature. High-resolution transmission electron microscopy (HRTEM) images were recorded from a JEOL-2100 (JEOL, Japan) instrument, which was operated at 200 kV.

Cell Culture. Human breast cancer cell line (MCF-7) was cultured in the Dulbecco's modified Eagle's medium (DMEM) medium supplemented with 10 wt % fetal bovine serum (FBS), 100 units mL^{-1} of penicillin, and 100 mg mL^{-1} of streptomycin. Human mammary epithelial cell line/normal breast cell line (MCF-10A) was cultured in the DMEM/F12 medium supplemented with 5 wt % horse serum, 20 μg mL^{-1} epidermal growth factor, 0.5 μg mL^{-1}

DOI: 10.1021/acsami.5b00270
ACS Appl. Mater. Interfaces 2015, 7, 5574−5582

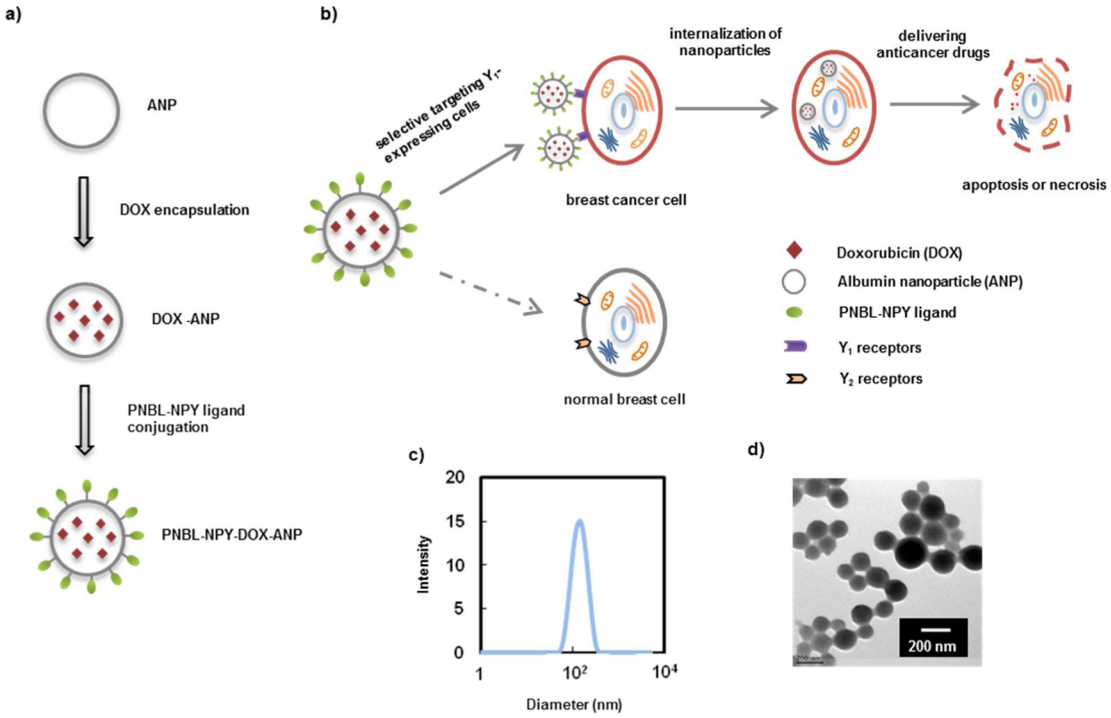

Figure 1. Schematic illustration of PNBL-NPY-DOX-ANP synthesis and characterization. (a) The scheme of PNBL-NPY-DOX-ANP synthesis. (b)The PNBL-NPY ligand-modified DOX-ANP could selectively target Y_1Rs-expressing human breast cancer cells and efficiently deliver the anticancer drug DOX-loaded nanoparticles into the cells. Because the normal breast tissue only expresses Y_2Rs, the PNBL-NPY modification could also reduce the damage to normal breast cells. (c) Size distributions of PNBL-NPY-DOX-ANP in PBS at room temperature measured by DLS at a scattering angle of 173° (backscatter detection). (d) HRTEM image of the synthesized PNBL-NPY-DOX-ANP.

hydrocortizone, 0.1 μg mL^{-1} choleratoxin, and 50 units mL^{-1} penicillin−streptomycin. The cells were incubated at 37 °C in a humidified atmosphere containing 5% CO_2.

Cellular Uptake of PNBL-NPY-DOX-ANP. For LSCM analysis, the six-well plates coated with 0.01% poly(Lys) were used for the experiment. MCF-7 (2.0 mL) or MCF-10A (2.0 mL) cells in complete DMEM or DMEM/F12 medium were seeded into each well at 5 × 10^4 cells mL^{-1} and allowed to adhere for 24 h at 37 °C in a humidified atmosphere containing 5% CO_2. The medium was then changed to a fresh nanoparticle solution containing 5 μg mL^{-1} DOX. After further 4 h of incubation, the cells were washed three times with PBS to remove any absorbed free nanoparticles. Afterward, the cells were fixed with 4% formaldehyde for 30 min, treated with 0.1% triton for 5 min, and then treated with 1.0% BSA for 30 min at room temperature. The actin of the cells and the nucleus of the cells were then stained with a mixture of rhodamine phalloidin (RP) and Hoechst 33342 for 30 min at room temperature. The samples were simultaneously excited at 350, 488, and 540 nm, and the fluorescent images at emission wavelengths 420−480, 500−540 and 600−660 nm were observed by an LSCM (TCS SP5 II, Leica, Germany).

For flow cytometry analysis, the six-well plates coated with 0.01% poly(Lys) were used for the experiment. 2.0 mL of MCF-7 or MCF-10A cells in complete DMEM or DMEM/F12 medium were seeded into each well at 5 × 10^4 cells mL^{-1} and allowed to adhere for 24 h at 37 °C in a humidified atmosphere containing 5% CO_2. The medium was then changed to a fresh nanoparticle solution containing 5 μg mL^{-1} DOX. After further 4 h of incubation, the cells were washed three times with PBS to remove any absorbed free nanoparticles. Afterward, the cells were washed three times with PBS and then harvested for further analysis. The mean fluorescence intensity (MFI) of cells (2 × 10^4 counts) were analyzed by flow cytometry (FACSCalibur, BD, USA), where the gate was arbitrarily set for the detection of green fluorescence (515−545 nm) with forward and side scattering dot plots used to discriminate cellular debris.

To investigate the selective cellular uptake of PNBL-NPY-DOX-ANP via Y_1Rs mediated endocytosis, MCF-7 cells were incubated with PNBL-NPY-DOX-ANP or DOX-ANP containing equivalent doxorubicin concentration in the presence or absence of PNBL-NPY (1 mM), respectively. After 4 h of incubation, the cells were washed three times with PBS and then harvested for further analysis. The MFI of cells (1 × 10^4 counts) were analyzed by flow cytometry, where the gate was arbitrarily set for the detection of green fluorescence (515−545 nm) with forward and side scattering dot plots used to discriminate cellular debris.

Cell Viability Assays. MCF-7 cells (100 μL) in complete DMEM medium were seeded into each well of a 96-well plate at a density of 1 × 10^5 cells mL^{-1} and allowed to adhere for 24 h at 37 °C in a humidified atmosphere containing 5% CO_2. The growth medium was replaced with 200 μL of fresh medium containing different DOX formulations investigated in this study, namely, DOX, ANP, DOX-ANP, and PNBL-NPY-DOX-ANP. Cells were washed with PBS after a brief incubation of 8 h, then 200 μL of fresh growth medium was added, and the cells were subsequently incubated for 64 h. Next, 10 μL of MTT (5 mg mL^{-1} in PBS) was added, and cells were incubated for an additional 4 h at 37 °C. After that, the growth medium was removed, and 100 μL of DMSO was added to each well to ensure solubilization of formazan crystals. The absorbance was recorded at a wavelength of 550 nm using an automated plate reader (iMark (168−1130), Biorad, U.S.). The cell viability was expressed as percentage calculated with the absorbance obtained from control well without drug treatment by using the following equation.

$$\text{viability}(\%) = (\text{Abst}/\text{Absc}) \times 100\%$$

where Abst is the absorbance of drug-treated well, and Absc is the absorbance of control well without drug treatment.

RESULTS AND DISCUSSION

Synthesis and Characterization of PNBL-NPY Modified DOX-ANP. The DOX-encapsulating ANP was prepared as in the previous method by encapsulating the DOX into ANP during the desolvation process of albumin.[25,31] Afterward, the

DOI: 10.1021/acsami.5b00270
ACS Appl. Mater. Interfaces 2015, 7, 5574−5582

Table 1. Effect of PNBL-NPY Ligand Amount on the Conjugation

sample no.	PNBL-NPY (mg)	PNBL-NPY to DOX-ANP feed ratio (μg mg^{-1})	conjugated PNBL-NPY amounts on surface (μg mg^{-1})	reaction ratio (%)	size (nm)	PDI	Zeta potential (mV)	stability of 7 d[a]	stability of one month
1	0.05	5.6	5.2	78.6	115.2	0.131	−32.3	−	−
2	0.1	11.1	10.7	86.7	113.4	0.106	−32.1	−	−
3	0.5	55.6	55.1	96.7	111.6	0.133	−28.0	−	−
4	1.0	111.1	110.6	96.1	141.9	0.248	−28.5	−	146.0
5	2.0	222.2	220.7	90.6	160.7	0.365	−28.9	+	+
6	5.0	555.6	428.4	93.4	447.4	0.687	−25.4	+	+

[a]− no aggregation and participation observed; + aggregation and participation observed.

PNBL-NPY ligands were conjugated to the surface of the ANP (Figure 1a). To avoid affecting the biological activity of PNBL-NPY, the carboxylic groups of ANP were activated by EDAC and NHS and then reacted with amine groups of PNBL-NPY, because the biological active site of PNBL-NPY to Y_1 receptors is located on its C-terminus.[35] As the conjugation amount of PNBL-NPY might affect the stability of the prepared nanoparticles, different amounts of PNBL-NPY were checked in our conjugation experiment (Table1). After reaction, the unreacted PNBL-NPY was determined by an HPLC-UV method at a wavelength of 220 nm (Supporting Information, Figure S2). We found that the water solubility and stability of PNBL-NPY-DOX-ANP were strongly affected by the amount of PNBL-NPY. The mean particle size of the PNBL-NPY-DOX-ANP was increased from 115.2 to 447.4 nm, when the amount of PNBL-NPY varied from 0.05 to 5.0 mg. The aggregation and participation were observed when the feed ratio of PNBL-NPY/DOX-ANP (w/w) was above 222.2 μg mg^{-1}. In the end, 111.1 μg mg^{-1} of PNBL-NPY was used for the preparation of PNBL-NPY-DOX-ANP, of which the PNBL-NPY conjugation ratio to DOX-ANP was 110.4 μg mg^{-1}. A UV method was used to determine the DOX amount encapsulated inside the ANP at a wavelength of 480 nm (Supporting Information, Figure S3). The drug loading content (DLC) and drug loading efficiency (DLE) were calculated with equations in the Experimental Section. In our study, the DLC and DLE were 2.57% and 86.5%, respectively (Supporting Information, Table S1). The study of DLS shows the mean hydrodynamic sizes of 141.9 nm for PNBL-NPY-DOX-ANP, with a narrow size-distribution (polydispersity index (PDI) < 0.241, Figure 1c and Table 1). This size range of our prepared nanoparticles is in good agreement with the literature values for targeted delivery of anticancer drugs to tumor sites, of which the nanoparticle is in the size range of 50−200 nm.[36−40] The TEM photograph indicates the prepared nanoparticles are spherical in shape and uniform in size, of which the mean diameter was ∼140 nm (Figure 1d). At pH 7.4, the prepared nanoparticles (sample no. 4) have a negative zeta-potential of −28.5 mV, which is due to the carboxyl groups on the hydrophilic shell of the nanoparticles. They could be stable for one month storage in PBS at 4 °C, of which the size changes are within 5 nm, and there is no aggregation and participation observed during that time (Table 1).

Release Profiles of DOX from PNBL-NPY-DOX-ANP. The release of DOX from DOX-ANP or PNBL-NPY-DOX-ANP with or without 2.0 mg mL^{-1} trypsin was determined at 37 °C as previous method.[25,31] As shown in Figure 2, both DOX-ANP and PNBL-NPY-DOX-ANP have a similar release profiles of DOX in the absence of trypsin. About 7.2% of DOX release from the DOX-ANP and PNBL-NPY-DOX-ANP within

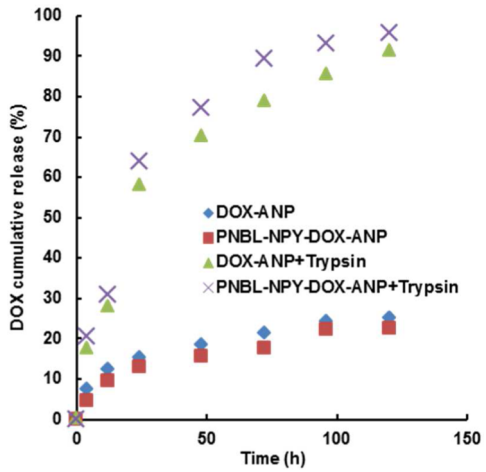

Figure 2. In vitro release profiles of DOX from the DOX-ANP or PNBL-NPY-DOX-ANP in PBS with or without 2.0 mg mL^{-1} trypsin at 37 °C.

4 h. In the end of the test, there is only ∼24.8% of DOX released in 120 h. This might be because the DOX was encapsulated inside the nanoparticles rather than physically absorbed on the surface, and the diffusion of DOX from the nanoparticles is slow.[25] However, in the presence of trypsin, the release of DOX from DOX-ANP and PNBL-NPY-DOX-ANP is dramatically enhanced, which was ∼95.8% in 120 h. This result indicates that the release of DOX from the nanoparticles is mainly caused by enzymatic degradation. In this case, the DOX can also be released from DOX-ANP or PNBL-NPY-DOX-ANP in cells due to the degradation of ANP by intracellular enzymes.[25,31]

Cellular Uptake of PNBL-NPY-DOX-ANP in MCF-7 Cells. Cellular uptake of the nanoparticles was assessed using a human breast cancer MCF-7 cell line previously shown to highly express Y_1Rs.[13,33] MCF-7 cells were incubated with PNBL-NPY modified and unmodified DOX-ANP in parallel for 4 h. LSCM images are shown in Figure 3, and the samples were simultaneously excited at 350, 488, and 540 nm. The cytoskeletons with rhodamine phalloidin (RP) (EX 540 nm, EM 600−660 nm) are red, and the nuclei stained with Hoechst (EX 350 nm, EM 420−480 nm) are blue. The fluorescent images of autofluorescent DOX-ANP and PNBL-NPY-DOX-ANP are green (EM 500−540 nm) at an excitation of 488 nm, and are red (EM 600−660 nm) at an excitation of 540 nm, so the yellow-colored nanoparticles are associated with the combination of green and red fluorescence emissions. Fluorescence emission spectra of DOX-ANP and PNBL-NPY-DOX-ANP at 488 and 540 nm are shown in Supporting Information, Figure S4. As shown in Figure 3, more PNBL-

DOI: 10.1021/acsami.5b00270
ACS Appl. Mater. Interfaces 2015, 7, 5574−5582

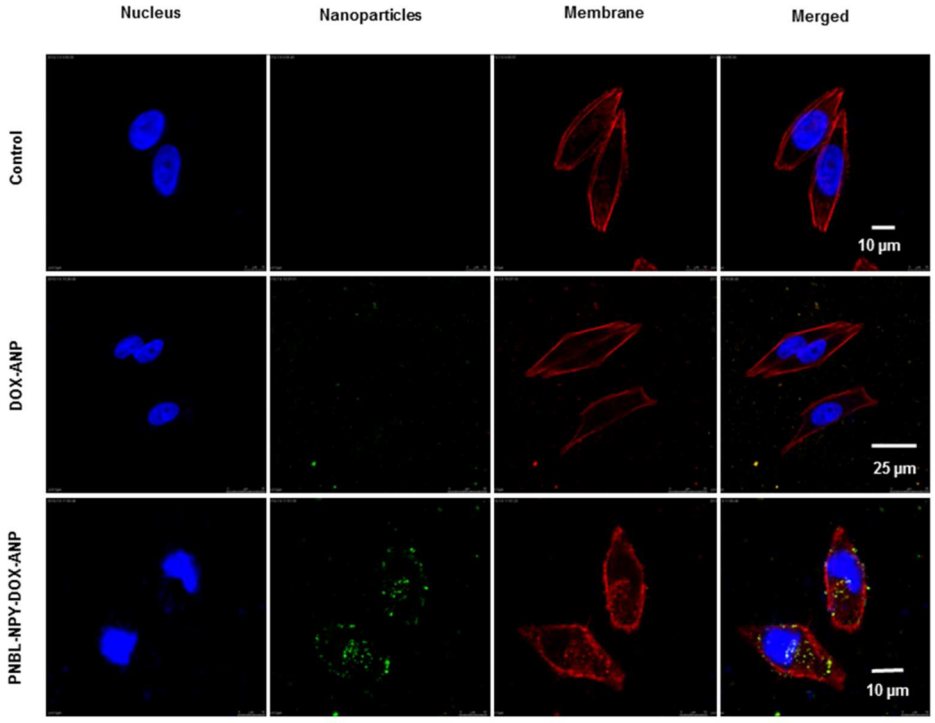

Figure 3. Cellular uptake of PNBL-NPY modified DOX-ANP in human breast cancer cells MCF-7. LSCM images of MCF-7 cells incubated with DOX-ANP and PNBL-NPY-DOX-ANP containing equivalent DOX concentration of 5 μg mL^{-1} for 4 h. The cytoskeletons with rhodamine phalloidin are red, the nuclei stained with hoechst are blue, and the nanoparticles are green and red (merged are yellow).

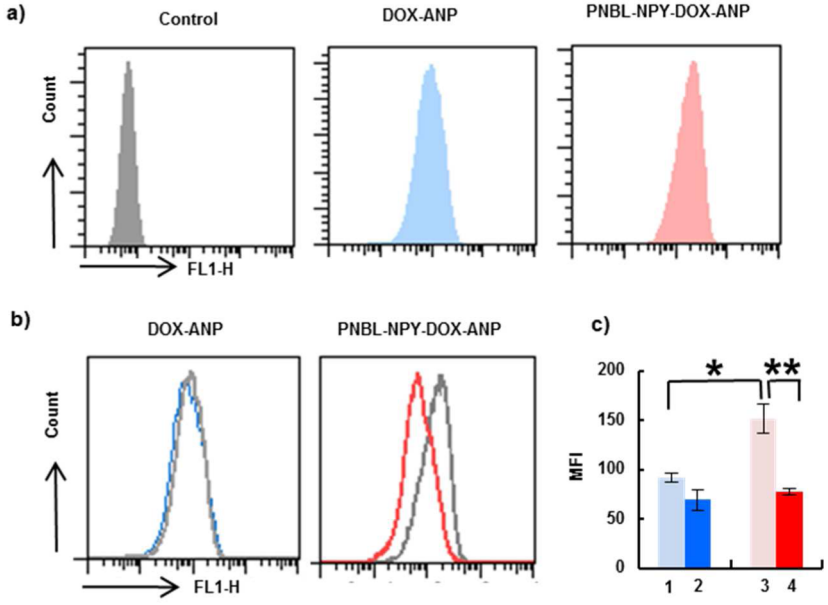

Figure 4. Flow cytometry analysis of MCF-7 cells incubated with DOX-ANP and PNBL-NPY-DOX-ANP. (a) MCF-7 cells incubate with DOX-ANP and PNBL-NPY-DOX-ANP containing equivalent DOX concentration of 10 μg mL^{-1} for 4 h. (b) MCF-7 cells were incubated with DOX-ANP and PNBL-NPY-DOX-ANP absence (gray line) or presence (color line) of 1 mM PNBL-NPY for 4 h. (c) Significant analysis of MFI for MCF-7 cells incubated with different nanoparticles. Data represent the mean ± SEM (n = 3,*P < 0.05, **P < 0.01). 1: DOX-ANP; 2: DOX-ANP with PNBL-NPY; 3: PNBL-NPY-DOX-ANP; 4: PNBL-NPY-DOX-ANP with PNBL-NPY.

NPY-DOX-ANP are internalized into MCF-7 cells than DOX-ANP. Consistently, the flow cytometry analysis (EX 488 nm, EM 515−545 nm, FL1-H) verified that PNBL-NPY-DOX-ANP treated MCF-7 cells showed much stronger mean fluorescence intensity (MFI) than DOX-ANP, which was 151.7 and 91.5, respectively (Figure 4a,c). The MFI of PNBL-NPY-DOX-ANP was significantly higher than that of the DOX-ANP, which was ~65.8% (P < 0.05). These results indicate that the modification of PNBL-NPY ligand could significantly improve the delivery of DOX-ANP into the MCF-7 cells. We also calculated the percentage of MCF-7 cell population that was able to internalize the PNBL-NPY modified or unmodified DOX-ANP. It was found that ~97.2% of MCF-7 cells were able to internalize the PNBL-NPY modified DOX-ANP, while only

DOI: 10.1021/acsami.5b00270
ACS Appl. Mater. Interfaces 2015, 7, 5574−5582

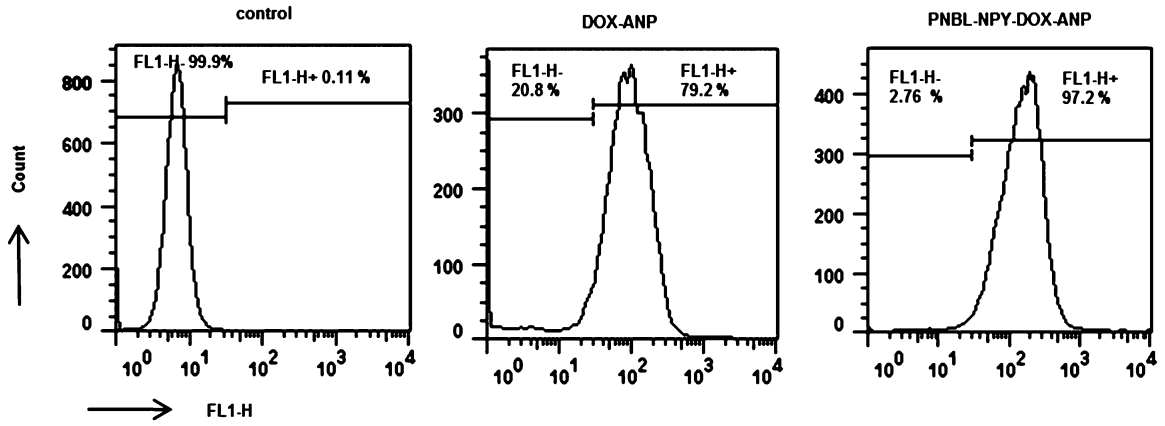

Figure 5. Percentage of MCF-7 cell population that was able to internalize the PNBL-NPY modified or unmodified DOX-ANP. MCF-7 cells incubated with DOX-ANP and PNBL-NPY-DOX-ANP containing equivalent DOX concentration of 10 μg mL^{-1} for 4 h. 10 000 MCF-7 cells were counted for each sample in the flow cytometry analysis.

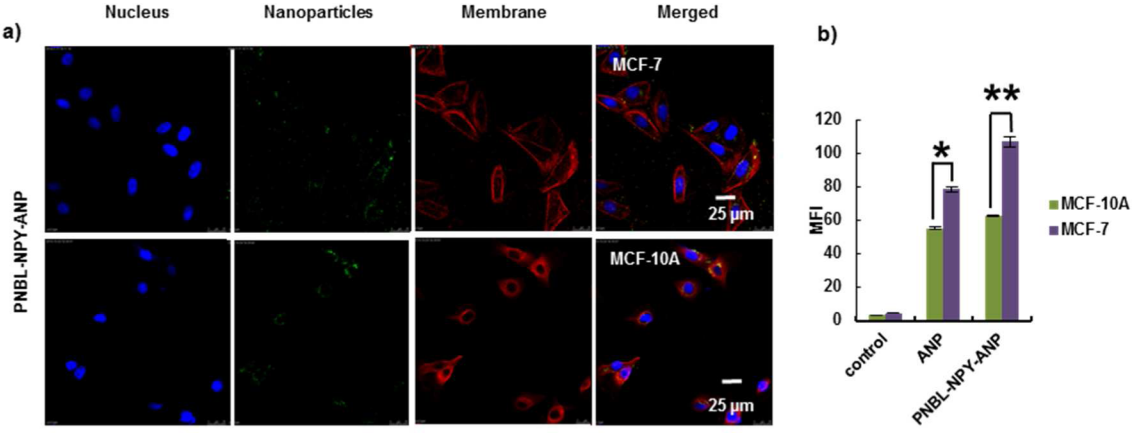

Figure 6. Comparison of cellular uptake difference between MCF-7 and MCF-10A cells. (a) LSCM images of MCF-7 and MCF-10A cells incubated with 0.25 mg mL^{-1} PNBL-NPY-ANP for 4 h. The cytoskeletons with rhodamine phalloidin are red, the nuclei stained with Hoechst are blue, and the nanoparticles are green and red (merged are yellow). (b) Flow cytometry analysis of MFI for MCF-7 and MCF-10A cells incubated with ANP or PNBL-NPY-ANP. Data represent the mean ± SEM (n = 3, * P < 0.05, ** P < 0.01).

79.2% of MCF-7 cells were able to uptake the DOX-ANP (Figure 5). In addition, MCF-7 cells was incubated with different concentration of the PNBL-NPY-DOX-ANP for 4 h, the MFI of MCF-7 cells showed a concentration-dependent increase, when PNBL-NPY-DOX-ANP concentration was increased from 0.25 to 1.0 mg mL^{-1} (Supporting Information, Figure S5). Our findings agree well with the previous reports that the NPY receptors internalization is only induced by agonists, because the PNBL-NPY ligand used in our study is an agonist of NPY receptors.[35,41,42]

To investigate whether cellular uptake of PNBL-NPY-DOX-ANP occurred via Y_1Rs-mediated endocytosis or not, MCF-7 cells were further incubated with PNBL-NPY-DOX-ANP and DOX-ANP in the presence or absence of 1 mM PNBL-NPY ligand for 4 h. Flow cytometry analysis showed that the presence of PNBL-NPY ligand had almost no effect on MFI of MCF-7 cells incubated with DOX-ANP, but it did significantly decrease the MFI of MCF-7 cells incubated with PNBL-NPY-DOX-ANP, of which the MFI was decreased from 151.7 to 77.2 (Figure 4b,c). This is because free PNBL-NPY ligand could competitively bind to Y_1R_S on MCF-7 cells and inhibit the cellular uptake of PNBL-NPY-DOX-ANP into the cells. The result indicates that the cellular uptake of PNBL-NPY-DOX-ANP is selectively mediated by Y_1Rs expressed on MCF-7 cells.

Cellular Uptake Difference between MCF-7 and MCF-10A Cells. Because Y_1Rs are overexpressed on human breast tumors, while normal human breast express Y_2Rs preferentially,[13,34] it is interesting to know whether PNBL-NPY modification could change the cellular uptake of nanoparticles between human breast cancer cells and human normal breast cells (human mammary epithelial cells). To check the cellular uptake difference, PNBL-NPY-modified ANP without DOX loading were used, because the normal breast cell MCF-10A is too sensitive to anticancer drug DOX. As shown in the LSCM images of MCF-7 and MCF-10A cells (Figure 6a), more PNBL-NPY-ANP is internalized into the MCF-7 cells than into the MCF-10A cells. Further flow cytometry analysis verifies that PNBL-NPY-ANP-treated MCF-7 cells have much stronger MFI than MCF-10A cells, which is 107.3 and 63.0, respectively (Figure 6b). The MFI of MCF-7 cells is significantly higher than that of MCF-10A cells (by ~70.4% (P < 0.01)). Compare to the unmodified ANP, the MFI of MCF-7 cells increased by 35.6% after the PNBL-NPY modification, but the MFI of MCF-10A cells changed only 13.2%. This result is due to the higher affinity of PNBL-NPY to Y_1Rs, but the affinity of PNBL-NPY to Y_2Rs is much lower.[32] This suggests that after the modification of PNBL-NPY ligand, drug carrier ANP prefers the breast cancer cell MCF-7 rather than the normal breast cell

DOI: 10.1021/acsami.5b00270
ACS Appl. Mater. Interfaces 2015, 7, 5574−5582

MCF-10A, by which the delivery of anticancer drug to normal breast cells could be reduced.

Cell Viability Testing for MCF-7 Cells. To address whether PNBL-NPY-modified DOX-ANP could be used for breast cancer therapy, the cytotoxicity of the prepared nanoparticles was evaluated by MTT assays for human breast cancer cells MCF-7. The MCF-7 cells were incubated with ANP and different formulation of DOX (equivalent DOX concentration 1 to 40 μg mL^{-1}) for 8 h, the growth medium was exchanged for a fresh one, and the cells were subsequently incubated for 64 h. As shown in Figure 7, there is no significant difference of cell viability between ANP and control sample, which means the material that we used for drug delivery has no cytotoxicity to the MCF-7 cells during this incubation time. However, the cell viability of MCF-7 cells incubated with PNBL-NPY-DOX-ANP is decreased when DOX concentration varies from 10 to 40 μg mL^{-1}, which is significantly lower than the DOX-ANP ($P < 0.05$) and the control sample ($P < 0.01$). This result indicates that the effective cytotoxicity of PNBL-NPY-DOX-ANP is significantly higher than that of the DOX-ANP. Therefore, the modification of PNBL-NPY not only promotes the delivery of DOX-ANP into MCF-7 cells but also efficiently inhibits the growth of MCF-7 cells in a concentration-dependent manner. As we see in Figure 7, the free DOX always induces a much lower cell viability compared to that of PNBL-NPY-DOX-ANP and DOX-ANP. This is mainly due to the fast diffusion of DOX to MCF-7 cells versus a sustained release of DOX from DOX-ANP. Our results are consistent with those reported in the literature, and the same phenomenon was observed when HeLa cells and HepG2 cells were incubated with DOX-encapsulating ANP and free DOX.[25,31] However, this situation might be improved, if dual drug loading was performed in our nanoparticle system. For example, two anticancer drugs, docetaxel and tamoxifen, have been loaded into poly(lactide)-D-α-tocopheryl poly(ethylene glycol succinate) (PLA-TPGS) nanoparticles, by which the drug antagonism was reduced and the cytotoxicity to MCF-7 cells was dramatically improved, comparing to single free drug or two free drugs in combination.[43]

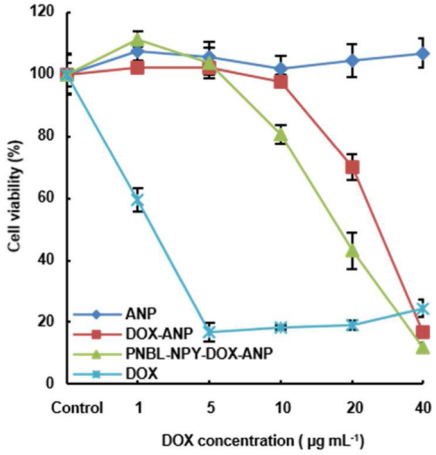

Figure 7. Cell viability test of human breast cancer cells MCF-7. MCF-7 cells incubated with different prepared nanoparticles containing equivalent DOX for 8 h, the growth medium was exchanged for a fresh one, and the cells were subsequently incubated for 64 h ($n = 5$ for each group). The x-axis is shown as DOX concentration encapsulated in nanoparticles. Bars correspond to mean ± SEM.

Effect of PNBL-NPY Ligand on MCF-7 Cells Growth. Previous studies have reported that neuropeptide Y and its analogues could affect the cell proliferation; for instance, neuropeptide Y could inhibit the growth of human neuronal epithelioma cells SK-N-MC.[13] To check whether the PNBL-NPY ligand has effect on the cell viability of human breast cancer cells MCF-7, MCF-7 cells were incubated with different concentration of PNBL-NPY ligand for 8 h, growth medium was exchanged for a fresh one, and the cells were subsequently incubated for 16 h. There was no significant effect observed when the concentration of PNBL-NPY was varied from 10 nM to 100 μM (Figure 8a). In our case, the concentration of PNBL-NPY conjugated to DOX-ANP was ~32 μM, so there was no significant effect of PNBL-NPY on MCF-7 cell viability observed for 24 h of incubation. However, when the incubation was prolonged to 72 h (Figure 8b), a significant inhibition of PNBL-NPY on the growth of MCF-7 cells was observed for all tested concentrations ($P < 0.01$). These results indicate that PNBL-NPY ligand could affect the growth of MCF-7 cells,

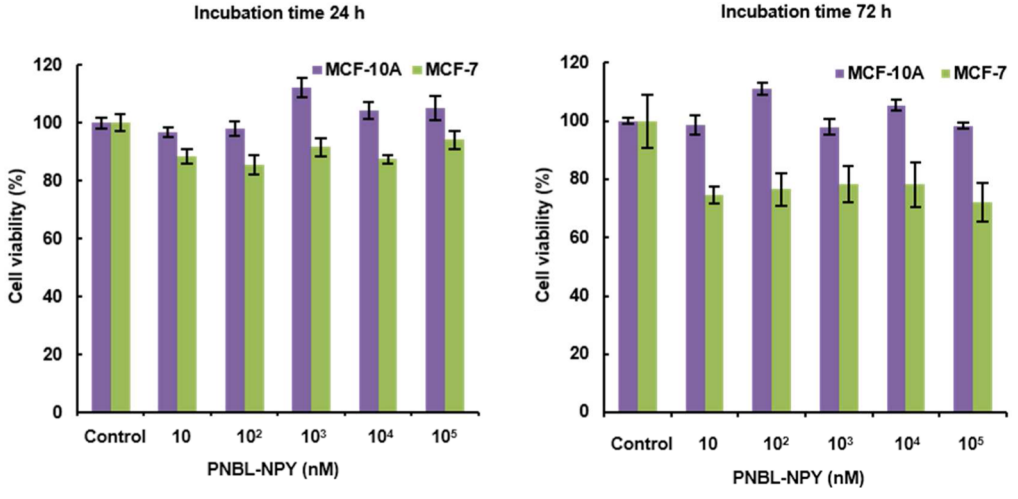

Figure 8. Effect of PNBL-NPY ligand on MCF-7 and MCF-10A cells growth. MCF-7 and MCF-10A cells were incubated with different concentration of PNBL-NPY ligand for 8 h, the growth medium was exchanged for a fresh one, and the cells were subsequently incubated for 16 h (a) and 64 h (b), respectively. Bars correspond to mean ± SEM ($n = 5$).

DOI: 10.1021/acsami.5b00270
ACS Appl. Mater. Interfaces 2015, 7, 5574−5582

which is highly dependant on the interaction time between PNBL-NPY ligand and the cells. Additionally, the effect of PNBL-NPY on the growth of MCF-10A cells was also tested in our lab under the same conditions. However, there is no significant effect observed for both 24 and 72 h of incubation (Figure 8). Therefore, the inhibition of PNBL-NPY-DOX-ANP on MCF-7 cells growth is not only induced by the anticancer drug DOX but also related to the synergistic effect of PNBL-NPY ligand.

Until now, most of the commerially available or clinically studied anticancer drugs loaded ANP are mainly based on the mechanism of enhanced permeability and retention (EPR) effect of tumors,[27−29,44] but our Y_1Rs-based nanoparticulate drug delivery system is able to actively target the breast cancer cells with high selectivity. Compared to traditional systemic administration of anticancer drugs through veins, our developed Y_1Rs-based nanoparticulate drug delivery system could be administrated multiply. Once the Y_1Rs ligand-induced cellular uptake difference between breast cancer cells and normal breast cells is as large as possible, the local application might be the best way to treat breast cancer in the early stage, without affecting the normal breast tissues or other organs. In the case of metastases, a systemic injection might be needed, due to the Y_1Rs being overexpressed in 100% of the examined metastases.[13] In the future, a multidisciplinary study should be encouraged; for example, the computer-aided drug design should be adopted to design a much better Y_1Rs ligand with extremely high Y_1Rs affinity and the lowest affinity to the Y_2Rs, providing Y_1Rs-based nanoparticulate drug delivery system the best selectivity and minimized side effects to normal tissues or organs.

CONCLUSIONS

In summary, we have demonstrated the use of Y_1Rs ligand, PNBL-NPY, as a targeted molecule to selectively deliver DOX-encapsulated biocompatible ANP to breast cancer cells and its potential for breast cancer therapy. Our findings reveal that PNBL-NPY can actively recognize and bind to the Y_1Rs that are significantly overexpressed on the surface of the breast cancer cells and selectively deliver DOX-ANP to human breast cancer cells MCF-7. This system is highly selective and able to distinguish the breast cancer cells from the normal cells, because normal breast cells express Y_2Rs only. Additionally, the enhanced targetability of PNBL-NPY-DOX-ANP might play an important role in the improvement of breast cancer therapy because of the following possible advantages: (i) improved delivery of DOX-ANP could transfer more DOX into breast cancer cells and induce a much stronger inhibition effect on the cells growth; (ii) PNBL-NPY ligand could generate a synergistic effect to inhibit the growth of breast cancer cells. Therefore, PNBL-NPY ligand could be used as a novel active targeted molecule to mediate the delivery of drug encapsulating nanoparticles into breast cancer cells with high selectivity and minimized damage to normal breast cells. This study may provide a guidance to develop new Y_1Rs-based nanoparticulate drug delivery system for a safer and more efficient breast cancer therapy.

ASSOCIATED CONTENT

Supporting Information

Mass spectrum of PNBL-NPY peptide; determination of PNBL-NPY concentration by HPLC; determination of DOX concentration; drug loading content and drug loading efficiency; fluorescence emission spectra of ANP, DOX-ANP, and PNBL-NPY-DOX-ANP; cellular uptake of MCF-7 cells incubated with difference concentration of PNBL-NPY-DOX-ANP. This material is available free of charge via the Internet at http://pubs.acs.org.

AUTHOR INFORMATION

Corresponding Author

*E-mail: aiguo@nimte.ac.cn. Phone: +86 574 86685039. Fax: +86 574 86685163.

Notes

The authors declare no competing financial interest.

ACKNOWLEDGMENTS

This work was supported by the Natural Science Foundation of China (Grant Nos. 51303196 and U1432114), Postdoctoral Science Foundation Grant of China (Grant No. 2013M531487), Ningbo Natural Science Foundation of China (Grant No. 2013A610092), and Hundred Talents Program of Chinese Academy of Sciences (WU A.G.). The authors also thank S. Gu from Zhejiang Univ. for helping MCF-10A cell culture, and L. Zheng from Ningbo Entry-Exit Inspection Quarantine Bureau of China for helping test the HPLC data.

REFERENCES

(1) Sawyers, C. Targeted Cancer Therapy. *Nature* **2004**, *432*, 294−297.
(2) Byrne, J. D.; Betancourt, T.; Brannon-Peppas, L. Active Targeting Schemes for Nanoparticle Systems in Cancer Therapeutics. *Adv. Drug Delivery Rev.* **2008**, *60*, 1615−1626.
(3) Kolhatkar, R.; Lote, A.; Khambati, H. Active Tumor Targeting of Nanomaterials using Folic Acid, Transferrin and Integrin Receptors. *Curr. Drug Discovery Technol.* **2011**, *8*, 197−206.
(4) Mi, Y.; Liu, Y.; Feng, S. S. Formulation of Docetaxel by Folic Acid-Conjugated d-Alpha-Tocopheryl Polyethylene Glycol Succinate 2000 (Vitamin E TPGS(2k)) Micelles for Targeted and Synergistic Chemotherapy. *Biomaterials* **2011**, *32*, 4058−4066.
(5) Hong, M.; Zhu, S.; Jiang, Y.; Tang, G.; Pei, Y. Efficient Tumor Targeting of Hydroxycamptothecin Loaded PEGylated Niosomes Modified with Transferrin. *J. Controlled Release* **2009**, *133*, 96−102.
(6) Onyuksel, H.; Mohanty, P. S.; Rubinstein, I. VIP-Grafted Sterically Stabilized Phospholipid Nanomicellar 17-Allylamino-17-Demethoxy Geldanamycin: A Novel Targeted Nanomedicine for Breast Cancer. *Int. J. Pharm.* **2009**, *365*, 157−161.
(7) Zhang, Y. F.; Wang, J. C.; Bian, D. Y.; Zhang, X.; Zhang, Q. Targeted Delivery of RGD-Modified Liposomes Encapsulating Both Combretastatin A-4 and Doxorubicin for Tumor Therapy: in Vitro and in Vivo Studies. *Eur. J. Pharm. Biopharm.* **2010**, *74*, 467−473.
(8) Xia, W.; Low, P. S. Folate-Targeted Therapies for Cancer. *J. Med. Chem.* **2010**, *53*, 6811−6824.
(9) Chen, Q.; Millar, H. J.; McCabe, F. L.; Manning, C. D.; Steeves, R.; Lai, K.; Kellogg, B.; Lutz, R. J.; Trikha, M.; Nakada, M. T.; Anderson, G. M. Alphav Integrin-Targeted Immunoconjugates Regress Established Human Tumors in Xenograft Models. *Clin. Cancer Res.* **2007**, *13*, 3689−3695.
(10) Reubi, J. C.; Laderach, U.; Waser, B.; Gebbers, J. O.; Robberecht, P.; Laissue, J. A. Vasoactive Intestinal Peptide/Pituitary Adenylate Cyclase-Activating Peptide Receptor Subtypes in Human Tumors and Their Tissues of Origin. *Cancer Res.* **2000**, *60*, 3105−3112.
(11) Gugger, M.; Reubi, J. C. Gastrin-Releasing Peptide Receptors in Non-Neoplastic and Neoplastic Human Breast. *Am. J. Pathol.* **1999**, *155*, 2067−2076.
(12) Korner, M.; Reubi, J. C. NPY Receptors in Human Cancer: A Review of Current Knowledge. *Peptides* **2007**, *28*, 419−425.

DOI: 10.1021/acsami.5b00270
ACS Appl. Mater. Interfaces 2015, 7, 5574−5582

(13) Reubi, J. C.; Gugger, M.; Waser, B.; Schaer, J. C. Y(1)-Mediated Effect of Neuropeptide Y in Cancer: Breast Carcinomas as Targets. *Cancer Res.* **2001**, *61*, 4636−4641.
(14) Khan, I. U.; Zwanziger, D.; Bohme, I.; Javed, M.; Naseer, H.; Hyder, S. W.; Beck-Sickinger, A. G. Breast-Cancer Diagnosis by Neuropeptide Y Analogues: from Synthesis to Clinical Application. *Angew. Chem., Int. Ed. Engl.* **2010**, *49*, 1155−1158.
(15) Guerin, B.; Dumulon-Perreault, V.; Tremblay, M. C.; Ait-Mohand, S.; Fournier, P.; Dubuc, C.; Authier, S.; Benard, F. [Lys(DOTA)4]BVD15, a Novel and Potent Neuropeptide Y Analog Designed for Y1 Receptor-Targeted Breast Tumor Imaging. *Bioorg. Med. Chem. Lett.* **2010**, *20*, 950−953.
(16) Zwanziger, D.; Khan, I. U.; Neundorf, I.; Sieger, S.; Lehmann, L.; Friebe, M.; Dinkelborg, L.; Beck-Sickinger, A. G. Novel Chemically Modified Analogues of Neuropeptide Y for Tumor Targeting. *Bioconjugate Chem.* **2008**, *19*, 1430−1438.
(17) Langer, M.; La Bella, R.; Garcia-Garayoa, E.; Beck-Sickinger, A. G. 99mTc-Labeled Neuropeptide Y Analogues as Potential Tumor Imaging Agents. *Bioconjugate Chem.* **2001**, *12*, 1028−1034.
(18) Peer, D.; Karp, J. M.; Hong, S.; Farokhzad, O. C.; Margalit, R.; Langer, R. Nanocarriers as an Emerging Platform for Cancer Therapy. *Nat. Nanotechnol.* **2007**, *2*, 751−760.
(19) Brannon-Peppas, L.; Blanchette, J. O. Nanoparticle and Targeted Systems for Cancer Therapy. *Adv. Drug Delivery Rev.* **2004**, *56*, 1649−1659.
(20) Wang, Y.; Cao, X. Y.; Guo, R.; Shen, M. W.; Zhang, M. G.; Zhu, M. F.; Shi, X. Y. Targeted Delivery of Doxorubicin into Cancer Cells Using a Folic Acid-Dendrimer Conjugate. *Polym. Chem.* **2011**, *2*, 1754−1760.
(21) Fu, F. F.; Wu, Y. L.; Zhu, J. Y.; Wen, S. H.; Shen, M. W.; Shi, X. Y. Multifunctional Lactobionic Acid-Modified Dendrimers for Targeted Drug Delivery to Liver Cancer Cells: Investigating the Role Played by PEG Spacer. *ACS Appl. Mater. Interfaces* **2014**, *6*, 16416−16425.
(22) Liu, W. N.; Wen, S. H.; Shen, M. W.; Shi, X. Y. Doxorubicin-Loaded Poly(Lactic-co-Glycolic Acid) Hollow Microcapsules for Targeted Drug Delivery to Cancer Cells. *New J. Chem.* **2014**, *38*, 3917−3924.
(23) Wu, Y. L.; Guo, R.; Wen, S. H.; Shen, M. W.; Zhu, M. F.; Wang, J. H.; Shi, X. Y. Folic Acid-Modified Laponite Nanodisks for Targeted Anticancer Drug Delivery. *J. Mater. Chem. B* **2014**, *2*, 7410−7418.
(24) Kratz, F. Albumin as a Drug Carrier: Design of Prodrugs, Drug Conjugates and Nanoparticles. *J. Controlled Release* **2008**, *132*, 171−183.
(25) Shen, Z.; Wei, W.; Tanaka, H.; Kohama, K.; Ma, G.; Dobashi, T.; Maki, Y.; Wang, H.; Bi, J.; Dai, S. A Galactosamine-Mediated Drug Delivery Carrier for Targeted Liver Cancer Therapy. *Pharmacol. Res.* **2011**, *64*, 410−419.
(26) Zhao, D.; Zhao, X.; Zu, Y.; Li, J.; Zhang, Y.; Jiang, R.; Zhang, Z. Preparation, Characterization, and in Vitro Targeted Delivery of Folate-Decorated Paclitaxel-Loaded Bovine Serum Albumin Nanoparticles. *Int. J. Nanomed.* **2010**, *5*, 669−677.
(27) Vis, A. N.; van der Gaast, A.; van Rhijn, B. W. G.; Catsburg, T. K.; Schmidt, C.; Mickisch, G. H. J. A Phase II Trial of Methotrexate-Human Serum Albumin (MTX-HSA) in Patients With Metastatic Renal Cell Carcinoma Who Progressed under Immunotherapy. *Cancer Chemother. Pharmacol.* **2002**, *49*, 342−345.
(28) Kratz, F. DOXO-EMCH (INNO-206): The First Albumin-Binding Prodrug of Doxorubicin to Enter Clinical Trials. *Expert Opin. Invest. Drugs* **2007**, *16*, 855−866.
(29) Gradishar, W. J.; Tjulandin, S.; Davidson, N.; Shaw, H.; Desai, N.; Bhar, P.; Hawkins, M.; O'Shaughnessy, J. Phase III Trial of nanoparticle Albumin-Bound Paclitaxel Compared with Polyethylated Castor Oil-Based Paclitaxel in Women with Breast Cancer. *J. Clin. Oncol.* **2005**, *23*, 7794−7803.
(30) Ma, X. H.; Gong, A.; Xiang, L. C.; Chen, T. X.; Gao, Y. X.; Liang, X. J.; Shen, Z. Y.; Wu, A. G. Biocompatible Composite Nanoparticles with Large Longitudinal Relaxivity for Targeted Imaging and Early Diagnosis of Cancer. *J. Mater. Chem. B* **2013**, *1*, 3419−3428.
(31) Shen, Z. Y.; Li, Y.; Kohama, K.; Oneill, B.; Bi, J. X. Improved Drug Targeting of Cancer Cells by Utilizing Actively Targetable Folic Acid-Conjugated Albumin Nanospheres. *Pharmacol. Res.* **2011**, *63*, 51−58.
(32) Zwanziger, D.; Bohme, I.; Lindner, D.; Beck-Sickinger, A. G. First Sselective Agonist of The Neuropeptide Y1-Receptor with Reduced Size. *J. Pept. Sci.* **2009**, *15*, 856−866.
(33) Amlal, H.; Faroqui, S.; Balasubramaniam, A.; Sheriff, S. Estrogen Up-Regulates Neuropeptide Y Y_1 Receptor Expression in a Human Breast Cancer Cell Line. *Cancer Res.* **2006**, *66*, 3706−3714.
(34) Nagaraja, G. M.; Othman, M.; Fox, B. P.; Alsaber, R.; Pellegrino, C. M.; Zeng, Y.; Khanna, R.; Tamburini, P.; Swaroop, A.; Kandpal, R. P. Gene Expression Signatures and Biomarkers of Noninvasive and Invasive Breast Cancer Cells: Comprehensive Profiles by Representational Difference Analysis, Microarrays and Proteomics. *Oncogene* **2006**, *25*, 2328−2338.
(35) Bohme, I.; Stichel, J.; Walther, C.; Morl, K.; Beck-Sickinger, A. G. Agonist Induced Receptor Internalization of Neuropeptide Y Receptor Subtypes Depends on Third Intracellular Loop and C-Terminus. *Cell. Signalling* **2008**, *20*, 1740−1749.
(36) Kim, J.; Lee, Y. M.; Kang, Y.; Kim, W. J. Tumor-Homing, Size-Tunable Clustered Nanoparticles for Anticancer Therapeutics. *ACS Nano* **2014**, *8*, 9358−9367.
(37) Albanese, A.; Tang, P. S.; Chan, W. C. The Effect of Nanoparticle Size, Shape, and Surface Chemistry on Biological Systems. *Annu. Rev. Biomed. Eng.* **2012**, *14*, 1−16.
(38) De Jong, W. H.; Hagens, W. I.; Krystek, P.; Burger, M. C.; Sips, A. J.; Geertsma, R. E. Particle Size-Dependent Organ Distribution of Gold Nanoparticles after Intravenous Administration. *Biomaterials* **2008**, *29*, 1912−1919.
(39) Kim, H.; Lee, D.; Kim, J.; Kim, T. I.; Kim, W. J. Photothermally Triggered Cytosolic Drug Delivery via Endosome Disruption Using a Functionalized Reduced Graphene Oxide. *ACS Nano* **2013**, *7*, 6735−6746.
(40) Kim, J.; Park, J.; Kim, H.; Singha, K.; Kim, W. J. Transfection and Intracellular Trafficking Properties of Carbon Dot-Gold Nanoparticle Molecular Assembly Conjugated with PEI-pDNA. *Biomaterials* **2013**, *34*, 7168−7180.
(41) Parker, S. L.; Parker, M. S.; Lundell, I.; Balasubramaniam, A.; Buschauer, A.; Kane, J. K.; Yalcin, A.; Berglund, M. M. Agonist Internalization by Cloned Y1 Neuropeptide Y (NPY) Receptor in Chinese Hamster Ovary Cells Shows Strong Preference for NPY, Endosome-Linked Entry and Fast Receptor Recycling. *Regul. Pept.* **2002**, *107*, 49−62.
(42) Parker, S. L.; Kane, J. K.; Parker, M. S.; Berglund, M. M.; Lundell, I. A.; Li, M. D. Cloned Neuropeptide Y (NPY) Y1 and Pancreatic Polypeptide Y4 Receptors Expressed in Chinese Hamster Ovary Cells Show Considerable Agonist-Driven Internalization, in Contrast to the NPY Y2 Receptor. *Eur. J. Biochem.* **2001**, *268*, 877−886.
(43) Tan, G. R.; Feng, S. S.; Leong, D. T. The Reduction of Anti-Cancer Drug Antagonism by the Spatial Protection of Drugs with PLA-TPGS Nanoparticles. *Biomaterials* **2014**, *35*, 3044−3051.
(44) Fang, J.; Nakamura, H.; Maeda, H. The EPR effect: Unique Features of Tumor Blood Vessels for Drug Delivery, Factors Involved, and Limitations and Augmentation of the Effect. *Adv. Drug Delivery Rev.* **2011**, *63*, 136−151.

DOI: 10.1021/acsami.5b00270
ACS Appl. Mater. Interfaces 2015, 7, 5574−5582